2014 IEEE International Conference on Robotics & Automation (ICRA)
Hong Kong Convention and Exhibition Center
May 31 - June 7, 2014. Hong Kong, China

Robotic Cell Manipulation Using Optical Tweezers with Limited FOV

X. Li, C. C. Cheah, X. Yan, and D. Sun

Abstract— **Microscopic optics and cameras are commonly used in micromanipulation or biomanipulation workstations since they provide a large spectrum of visual details and information. The visual feedback information also improves robustness to uncertainty and accuracy of micromanipulation. Among various micromanipulation systems, optical tweezers are one of the most useful instruments that utilize a focused beam of light to manipulate biological cell or nanoparticles without physical contact. However, current optical manipulation techniques fail if the laser beam is not within the field of view (FOV) of the microscope. To solve this problem, we present a robotic control technique for optical manipulation with limited FOV of microscope. The proposed control strategy consists of a vision based control that manipulates the trapped cell to move to a desired position inside the FOV and a Cartesian-space feedback control that drives the laser beam back when it is outside the FOV. Thus, the proposed method allows the laser beam to leave the FOV during the course of manipulation and the transition from one feedback to another is smooth. The stability of the closed-loop system is analysed by using Lyapunov-like methods, with consideration of the dynamic interaction between the cell and the manipulator of the laser source. Experimental results are presented to illustrate the performance of the proposed method.**

I. Introduction

With the rapid advances in sensor technologies and the integration of robotic and biomedical technologies at micro and nano scales, a variety of vision-based robotic micromanipulation systems have been developed in biological or biomedical engineering [1]–[4].

Among various micromanipulators, optical tweezers [5] have been extensively used in micromanipulation because of its ability of manipulating biological cell or nano particles without physical contact. Over the past years, several robotic control techniques have been introduced for optical tweezers to improve the efficiency of optical manipulation [6]–[15]. A comparison between the performance of several classic control methods for optical manipulation was given in [6]. In [7], a proportional-gain feedback controller was implemented on optical tweezers. In [8], a weighted-recursive-least-square algorithm was proposed for real-time calibration and estimation of system parameters. A minimum variance control method was proposed to minimize the Brownian motion of an optically trapped probe in [9]. In [10], a simple setpoint controller was proposed to manipulate the single cell to a desired position. In [11], a PID feedback controller and a synchronization control strategy were developed for automatic transportation of biological cells. In [12], an adaptive disturbance observer was developed for dynamic force sensing in an optical trap. To manipulate multiple cells to a desired region, a region reaching control method was presented in [13]. In [14], a dynamic viscous drag force method was utilized to characterize the force exerted on a trapped cell, and then a modified A-star path planning algorithm was proposed for cell transportation. A simultaneous trapping and manipulation technique was proposed for optical tweezers in [15], which allows the laser beam to automatically trap then manipulate the cell when it is not within the optical trap.

In an optical tweezers system, the position of cell can only be specified in image space inside the FOV of microscope, and the visual feedback of the position of cell is required for the closed-loop control of the laser beam. Therefore, the position of laser in the optical tweezers system is also specified in image space, and the laser beam should be controlled to stay within the FOV. While a high-resolution microscope is required to guarantee the accuracy of optical manipulation, the FOV is quite limited and existing optical manipulation methods [6]–[15] fail when the laser beam starts outside the FOV or leaves the FOV during the course of manipulation. While several research works have been reported in the literature of vision-based robot control with limited FOV [16]–[18], the problem of optical manipulation with limited FOV has not been systematically solved.

In this paper, a new robotic manipulation technique is proposed for optical manipulation with limited FOV. The proposed controller consists of a vision-based control that ensures the manipulation of the trapped cell to the desired position inside the FOV and a Cartesian-space feedback control that drives the laser beam back to the FOV of microscope when it is outside. The use of feedback information that transits smoothly between Cartesian space and vision space, allows the laser beam to leave the FOV during the course of manipulation. The proposed controller is based on the dynamic formulation where the position of laser source is controlled by closed-loop robotic manipulation techniques. The stability of the overall system is analyzed by using Lyapunov-like method, with consideration of the dynamic interactions between the manipulator of laser source and the biological cell. Experimental results are presented to illustrate the performance of the proposed cell manipulation method with limited FOV.

X. Li, C. C. Cheah, and X. Yan are with the School of Electrical and Electronic Engineering, Nanyang Technological University, Singapore. D. Sun is with the Department of Mechanical and Biomedical Engineering, City University of Hong Kong, Hong Kong. The work of the first three authors was supported by the Agency For Science, Technology And Research of Singapore (A*STAR), (reference 1121202014), and the work of the last author was supported in part by the Hong Kong University Grants Council (UGC) Special Equipment Grant (SET_CityU 01).

II. Optical Tweezers System

The basic principle of optical trap is based on the transfer of momentum from photons to microscopic objects, when a focused beam of light passes through the object that is immersed in a medium. The refraction of the photons at the boundary between the object and the medium, results in a stable trap of the object [5].

Optical tweezers are the scientific instruments based on the optical trap, which can manipulate the microscopic objects without physical contact. The main features consist of a large numerical aperture oil-immersion objective, a standard phase contrast microscope illumination, and a CCD camera. The laser beam is directed into the epifluorescence port of the microscope and then introduced to the microscope's optical path using a dichroic mirror located in the cube turret.

A. Dynamic Model of Biological Cell and Manipulator

The dynamic model of the cell in an optical tweezers system is described by the following equation [19]:

$$\boldsymbol{M}\ddot{\boldsymbol{x}} + \boldsymbol{B}\dot{\boldsymbol{x}} + k(\boldsymbol{x} - \boldsymbol{p}) = \boldsymbol{0}, \tag{1}$$

where $\boldsymbol{x} = [x_1, x_2]^T \in \Re^2$ is the position of cell, and $\boldsymbol{p} = [p_1, p_2]^T \in \Re^2$ is the position of laser, $\boldsymbol{M} \in \Re^{2\times 2}$ denotes the mass matrix which is diagonal and positive definite, $\boldsymbol{B} \in \Re^{2\times 2}$ represents the friction matrix which is also diagonal and positive definite, and k denotes the trapping stiffness which is constant when the cell is located in a small neighborhood of the centroid of the focused laser beam [10], [11], [13]. Both $\boldsymbol{x}$ and $\boldsymbol{p}$ are specified in image space of microscope. Since the FOV is limited, the positions of laser and cell in image space are only available within the FOV.

In this paper, the position of the laser beam $\boldsymbol{p}$ is controlled by closed-loop robotic manipulation techniques. When a linear motorized stage is used as a manipulator, the dynamic model is specified as [15]:

$$\boldsymbol{M}_q\ddot{\boldsymbol{q}} + \boldsymbol{B}_q\dot{\boldsymbol{q}} = \boldsymbol{u}, \tag{2}$$

where $\boldsymbol{q} \in \Re^n$ is the position of laser beam in Cartesian space, $\boldsymbol{M}_q$ is the mass matrix which is diagonal and positive definite, $\boldsymbol{B}_q$ represents the friction matrix which is also diagonal and positive definite, and $\boldsymbol{u}$ denotes the control input which is the force exerted on the manipulator. The dynamic model described by equation (2) can be parameterized as: $\boldsymbol{M}_q\ddot{\boldsymbol{q}} + \boldsymbol{B}_q\dot{\boldsymbol{q}} = \boldsymbol{Y}_q(\dot{\boldsymbol{q}}, \ddot{\boldsymbol{q}})\boldsymbol{\theta}_q$, where $\boldsymbol{Y}_q(\dot{\boldsymbol{q}}, \ddot{\boldsymbol{q}})$ is a known regressor matrix, and $\boldsymbol{\theta}_q = [\theta_{q1}, \cdots, \theta_{qn_q}]^T$ represents a set of dynamic parameters.

B. Camera Model

In optical tweezers system, the relationship between the robot frame and the camera is to be derived. The pinhole camera model [20], [21] is widely used to represent the mapping from Cartesian space to image space. Based on the pinhole camera model, the velocity of the image feature is related to the velocity of the feature point in Cartesian space by using the image Jacobian matrix. The image-space velocity of laser beam is related to the velocity of laser beam in Cartesian space as:

$$\dot{\boldsymbol{p}} = \boldsymbol{J}_I(\boldsymbol{q})\dot{\boldsymbol{q}}, \tag{3}$$

where $\boldsymbol{J}_I(\boldsymbol{q})$ is the image Jacobian matrix [22], [23], $\dot{\boldsymbol{p}}$ is the velocity of laser beam in image space, and $\dot{\boldsymbol{q}}$ is the velocity of laser beam in Cartesian space. While the position of laser beam in Cartesian space $\boldsymbol{q}$ is measured by encoders, the position of laser beam in image space $\boldsymbol{p}$ can only be obtained with image processing techniques within the FOV.

III. Optical Manipulation with Limited FOV

Since the FOV of microscope is limited, the optical manipulation fails when the laser beam leaves the FOV. To solve the problem of limited FOV, a new robot control method is proposed for optical manipulation of biological cell in this section, which allows the laser beam to transit smoothly outside or inside the FOV of microscope.

The main idea is to divide the entire workspace into a Cartesian-space region and an image-space region as shown in Fig. 1. The image-space region is formulated to match the FOV and the Cartesian-space region is set slightly overlapped with the image-space region such that the laser beam does not get stuck when it transits between the image-space region and the Cartesian-space region.

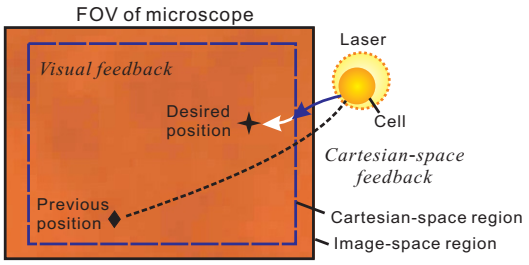

Fig. 1. The visual feedback is employed to guarantee the convergence of position error inside the FOV, while the Cartesian-space feedback is used to drive the laser beam back to the FOV when it leaves the FOV during the course of manipulation.

When the laser beam leaves the FOV during the course of manipulation due to overshoot or external perturbation, neither the cell nor the laser can be observed by the microscope. To solve the problem, the laser beam is firstly driven back to the FOV with Cartesian-space feedback. After the laser beam moves back into the FOV, that is, inside the image-space region, the visual feedback is then activated and employed to transport the trapped cell to the desired position.

The development of control strategy follows a backstepping procedure. First, a desired position input for the laser beam $\boldsymbol{p}_d$ is specified in image space to guarantee the convergence of position error. Next, a control input for the manipulator of laser beam is derived with regional feedback from Cartesian space and image space respectively, to ensure that the actual position of laser beam $\boldsymbol{p}$ tracks the desired position input $\boldsymbol{p}_d$ such that $\Delta\boldsymbol{p} = \boldsymbol{p} - \boldsymbol{p}_d \to \boldsymbol{0}$.

A. Desired Position Input of Laser Source

The desired position input for the laser is proposed as:

$$\boldsymbol{p}_d = \boldsymbol{x} - k^{-1}\boldsymbol{K}_p\Delta\boldsymbol{x} - k^{-1}\boldsymbol{K}_d\dot{\boldsymbol{x}}, \tag{4}$$

where $\boldsymbol{K}_p$ and $\boldsymbol{K}_d$ are diagonal and positive definite, and $\Delta\boldsymbol{x} = \boldsymbol{x} - \boldsymbol{x}_d$ where $\boldsymbol{x}_d$ is the desired position that can only be specified in image space.

Substituting the desired position input for the laser beam (4) into the dynamic equation of the cell, it is obtained:

$$\boldsymbol{M}\ddot{\boldsymbol{x}} + \boldsymbol{B}\dot{\boldsymbol{x}} + \boldsymbol{K}_p\Delta\boldsymbol{x} + \boldsymbol{K}_d\dot{\boldsymbol{x}} = k\Delta\boldsymbol{p}. \tag{5}$$

A Lyapunov-like candidate V_x is proposed as:

$$V_x = \tfrac{1}{2}\dot{\boldsymbol{x}}^T\boldsymbol{M}\dot{\boldsymbol{x}} + \tfrac{1}{2}\Delta\boldsymbol{x}^T\boldsymbol{K}_p\Delta\boldsymbol{x}. \tag{6}$$

Differentiating V_x with respect to time and substituting equation (5) into it, we have:

$$\begin{aligned}\dot{V}_x &= -\dot{\boldsymbol{x}}^T[(\boldsymbol{B}+\boldsymbol{K}_d)\dot{\boldsymbol{x}} + \boldsymbol{K}_p\Delta\boldsymbol{x} - k\Delta\boldsymbol{p}] + \dot{\boldsymbol{x}}^T\boldsymbol{K}_p\Delta\boldsymbol{x} \\ &= -\dot{\boldsymbol{x}}^T(\boldsymbol{B}+\boldsymbol{K}_d)\dot{\boldsymbol{x}} + k\dot{\boldsymbol{x}}^T\Delta\boldsymbol{p}.\end{aligned} \tag{7}$$

It can be shown that the position error $\Delta\boldsymbol{x}$ converges to zero when $\Delta\boldsymbol{p} = \boldsymbol{0}$. A control input for the manipulator of the laser source will be developed later to ensure the convergence of $\Delta\boldsymbol{p} \to \boldsymbol{0}$.

Remark 1: The desired position $\boldsymbol{x}_d$ is referred to the position of feature that can only be specified in image space. For example, in cell fusion [24], the desired position $\boldsymbol{x}_d$ is specified as the position of the cell that is to be fused, which can only be specified in image space. Since both the position of cell $\boldsymbol{x}$ and the desired position $\boldsymbol{x}_d$ are only available in image space, the desired position input $\boldsymbol{p}_d$ in equation (4) can only be specified inside the FOV as well. Position measurement obtained through image processing is usually slower than the use of encoders. Therefore, a smaller image-space region can be specified to cover the vicinity of the desired position only, instead of the entire FOV. △△△

B. Image-Space Region and Cartesian-Space Region

Since the desired position input is not available outside the FOV, the desired position input is redefined as:

$$\boldsymbol{p}_d = w(\boldsymbol{x} - k^{-1}\boldsymbol{K}_p\Delta\boldsymbol{x} - k^{-1}\boldsymbol{K}_d\dot{\boldsymbol{x}}), \tag{8}$$

where w is a weight factor [18]. The weight factor w=0 when the laser beam is outside the FOV, and it smoothly increases to 1 when the laser beam enters the FOV. Therefore, $\boldsymbol{p}_d$=0, and $\dot{\boldsymbol{p}}_d$=0 when the laser beam is outside the FOV and $\boldsymbol{p}_d$ is described by equation (4) when it is inside the FOV.

The image-space region consists of a task-oriented region $f_t(\boldsymbol{p})$ and a high-order region $f_h(\boldsymbol{p})$. First, a task-oriented region is introduced to enclose $\boldsymbol{p}_d$ as:

$$f_t(\boldsymbol{p}) = \frac{(p_1 - p_{d1})^2}{(p_{b1} - p_{d1})^2} + \frac{(p_2 - p_{d2})^2}{(p_{b2} - p_{d2})^2} - 1 \le 0, \tag{9}$$

where $\boldsymbol{p}_b = [p_{b1}, p_{b2}]^T \in \Re^2$ is the bound of the region. The region described by equation (9) represents a superellipse in image space, and the bounds are divided into four parts such that the desired position $\boldsymbol{p}_d$ is not necessary the centre of the superellipse.

The potential energy for the region $f_t(\boldsymbol{p})$ is introduced as:

$$P_t(\boldsymbol{p}) = \frac{k_t}{N}\{1 - [min(0, f_t(\boldsymbol{p}))]^N\}, \tag{10}$$

where k_t is a positive constant, and $N \ge 4$ is the order of the potential energy function which is also an even integer. Note that the bottom point of the potential energy corresponds to the desired position input $\boldsymbol{p}_d$, and thus the potential field of $P_t(\boldsymbol{p})$ drives the actual position of the laser beam $\boldsymbol{p}$ to track the desired position $\boldsymbol{p}_d$ such that $\Delta\boldsymbol{p} \to \boldsymbol{0}$.

The top contour of $P_t(\boldsymbol{p})$ is not a rectangle and varies as $\boldsymbol{p}_d$ is varying, which cannot match the FOV. Therefore, a high-order region is formulated to enclose $f_t(\boldsymbol{p}) \le 0$ as:

$$f_h(\boldsymbol{p}) = \frac{(p_1 - p_{d1})^{n_h}}{(p_{b1} - p_{d1})^{n_h}} + \frac{(p_2 - p_{d2})^{n_h}}{(p_{b2} - p_{d2})^{n_h}} - 1 \le 0, \tag{11}$$

where n_h is the order of the region function which is also an even integer. In general, $n_h \ge 20$ such that the high-order region $f_h(\boldsymbol{p})$ is specified as a rectangle with rounded corners which can match the fixed FOV. The potential energy for $f_h(\boldsymbol{p})$ is proposed as:

$$P_h(\boldsymbol{p}) = \frac{k_h}{N^2}\{min[0, [min(0, f_h(\boldsymbol{p}))]^N - (\kappa_h^{n_h} - 1)^N]\}^N, \tag{12}$$

where k_h is a positive constant, and $0 < \kappa_h < 1$ is a positive constant. The top contour of $P_h(\boldsymbol{p})$ corresponds to the region $f_h(\boldsymbol{p})$ which is a rectangle with rounded corners.

The overall potential energy in image space is defined as the summation of $P_t(\boldsymbol{p})$ and $P_h(\boldsymbol{p})$ as:

$$P_I(\boldsymbol{p}) = k_p\beta_x(P_t(\boldsymbol{p}) + P_h(\boldsymbol{p})), \tag{13}$$

where k_p and β_x are positive constants. The top contour of $P_I(\boldsymbol{p})$ is a rectangle with fixed contour that corresponds to the high-order region $f_h(\boldsymbol{p})$, and its bottom part is the desired position input $\boldsymbol{p}_d$. The combination of task-oriented region and high-order region not only matches the fixed rectangular FOV of microscope but also guarantees that the actual position of laser beam in image space $\boldsymbol{p}$ tracks the desired position input $\boldsymbol{p}_d$ after the laser beam enters the image-space region.

Partial differentiating the potential energy function $P_I(\boldsymbol{p})$ with respect to $\Delta\boldsymbol{p} = \boldsymbol{p} - \boldsymbol{p}_d$, the gradient of the potential energy is obtained respectively as:

$$(\frac{\partial P_I(\boldsymbol{p})}{\partial\Delta\boldsymbol{p}})^T = k_p\beta_x[(\frac{\partial P_t(\boldsymbol{p})}{\partial\Delta\boldsymbol{p}})^T + (\frac{\partial P_h(\boldsymbol{p})}{\partial\Delta\boldsymbol{p}})^T] \triangleq k_p\beta_x\Delta\boldsymbol{\varepsilon}_x, \tag{14}$$

where

$$\begin{aligned}(\frac{\partial P_h(\boldsymbol{p})}{\partial\Delta\boldsymbol{p}})^T = k_h\{&min\{0, [min(0, f_h(\boldsymbol{p}))]^N - \\ &(\kappa_h^{n_h} - 1)^N\}\}^{N-1}[min(0, f_h(\boldsymbol{p}))]^{N-1}(\frac{\partial f_h(\boldsymbol{p})}{\partial\Delta\boldsymbol{p}})^T,\end{aligned} \tag{15}$$

and

$$(\frac{\partial P_t(\boldsymbol{p})}{\partial\Delta\boldsymbol{p}})^T = -k_t[min(0, f_t(\boldsymbol{p}))]^{N-1}(\frac{\partial f_t(\boldsymbol{p})}{\partial\Delta\boldsymbol{p}})^T. \tag{16}$$

The vector $\Delta\boldsymbol{\varepsilon}_x$ is the image-space region error which is used to ensure the convergence of $\boldsymbol{p} \to \boldsymbol{p}_d$ inside the image-space region. Note that $\Delta\boldsymbol{\varepsilon}_x$ reduces to zero when the laser beam is outside the image-space region where $f_h(\boldsymbol{p}) > 0$. That is, the visual feedback is only activated after the laser beam enters the image-space region.

A Cartesian-space region is then introduced to drive the laser beam towards the image-space region if the laser beam leaves the FOV during the course of manipulation. Since the objective is to bring the laser beam into the image-space region, only the position of the laser beam is sufficient. Therefore, the Cartesian-space region is specified as:

$$\boldsymbol{f}_c(\boldsymbol{q})=\begin{bmatrix} f_{c1}(q_1) \\ f_{c2}(q_2) \\ f_{c3}(q_2) \end{bmatrix} = \begin{bmatrix} \frac{(q_1-q_{f1})^2}{(q_{b1}-q_{f1})^2}-1 \\ \frac{(q_2-q_{f2})^2}{(q_{b2}-q_{f2})^2}-1 \\ \frac{(q_3-q_{f3})^2}{(q_{b3}-q_{f3})^2}-1 \end{bmatrix} \geq \mathbf{0}, \quad (17)$$

where $\boldsymbol{q}_f=[q_{f1}, q_{f2}, q_{f3}]^T$ is a static reference position, and the vector $\boldsymbol{q}_b = [q_{b1}, q_{b2}, q_{b3}]^T$ denotes bounds of Cartesian-space region. When the function $\boldsymbol{f}_c(\boldsymbol{q})$ is mapped from Cartesian space to image space, it corresponds to a rectangle which can match the high-order image-space region $f_h(\boldsymbol{p})$. The Cartesian-space feedback is employed where $\boldsymbol{f}_c(\boldsymbol{q})\geq\mathbf{0}$.

The corresponding potential energy is defined as:

$$P_C(\boldsymbol{q})=k_p\beta_q \sum_{i=1}^{3} \frac{k_{ri}}{N}[max(0, f_{ci}(q_i))]^N, \quad (18)$$

where β_q and k_{ri} are positive constants. As seen from equation (18), $P_C(\boldsymbol{q})$ is smooth and lower-bounded by zero, and it automatically reduces to zero where $\boldsymbol{f}_c(\boldsymbol{q}) \leq \mathbf{0}$.

Similarly, partial differentiating the potential energy function $P_C(\boldsymbol{q})$ with respect to $\boldsymbol{q}$, the gradient is obtained as:

$$\begin{aligned}(\frac{\partial P_C(\boldsymbol{q})}{\partial \boldsymbol{q}})^T &= k_p\beta_q \sum_{i=1}^{3} k_{ri}[max(0, f_{ci}(q_i))]^{N-1}(\frac{\partial f_{ci}(q_i)}{\partial \boldsymbol{q}})^T \\ &\triangleq k_p\beta_q\Delta\boldsymbol{\varepsilon}_q, \end{aligned} \quad (19)$$

where $\Delta\boldsymbol{\varepsilon}_q$ denotes the Cartesian-space region error which drives the laser beam to transit from the Cartesian-space region to the image-space region, and it naturally reduces to zero after the laser beam leaves the Cartesian-space region. Different region error variables work in different local regions, and the combination of local feedback guarantees the realization of optical manipulation with limited FOV.

IV. Robotic Manipulation of Laser Source

Using the region errors in image space and Cartesian space, a robotic control strategy is developed for optical manipulation in this section. First, a sliding vector is introduced for the manipulator of laser source as:

$$\begin{aligned}\boldsymbol{s}_q &= \dot{\boldsymbol{q}} - \dot{\boldsymbol{q}}_r = \dot{\boldsymbol{q}} - \boldsymbol{J}_I^{+}(\boldsymbol{q})\dot{\boldsymbol{p}}_a \\ &+\beta_x\boldsymbol{J}_I^T(\boldsymbol{q})\Delta\boldsymbol{\varepsilon}_x+\beta_q\Delta\boldsymbol{\varepsilon}_q, \end{aligned} \quad (20)$$

where $\boldsymbol{J}_I^{+}(\boldsymbol{q})$ is the pseudo-inverse of $\boldsymbol{J}_I(\boldsymbol{q})$, and $\dot{\boldsymbol{p}}_a$ is a reference vector as: $\dot{\boldsymbol{p}}_a=[\dot{p}_{d1}\frac{p_{b1}-p_1}{p_{b1}-p_{d1}}, \dot{p}_{d2}\frac{p_{b2}-p_2}{p_{b2}-p_{d2}}]^T$.

Using the sliding vector $\boldsymbol{s}_q$, the dynamic model of the manipulator in equation (2) is rewritten as:

$$\boldsymbol{M}_q\dot{\boldsymbol{s}}_q+\boldsymbol{B}_q\boldsymbol{s}_q+\boldsymbol{Y}_q(\dot{\boldsymbol{q}}_r, \ddot{\boldsymbol{q}}_r)\boldsymbol{\theta}_q=\boldsymbol{u}. \quad (21)$$

The control input of the manipulator is proposed as:

$$\begin{aligned}\boldsymbol{u} &= -\boldsymbol{K}_s\boldsymbol{s}_q + \boldsymbol{Y}_q(\dot{\boldsymbol{q}}_r, \ddot{\boldsymbol{q}}_r)\hat{\boldsymbol{\theta}}_q \\ &-k_p(\beta_x\boldsymbol{J}_I^T(\boldsymbol{q})\Delta\boldsymbol{\varepsilon}_x+\beta_q\Delta\boldsymbol{\varepsilon}_q), \end{aligned} \quad (22)$$

where $\boldsymbol{K}_s$ is a diagonal and positive definite matrix, and the estimated parameters $\hat{\boldsymbol{\theta}}_q$ are updated as:

$$\dot{\hat{\boldsymbol{\theta}}}_q = -\boldsymbol{L}_q\boldsymbol{Y}_q^T(\dot{\boldsymbol{q}}_r, \ddot{\boldsymbol{q}}_r)\boldsymbol{s}_q, \quad (23)$$

where $\boldsymbol{L}_q$ is a positive definite matrix. The region errors $\Delta\boldsymbol{\varepsilon}_x$ and $\Delta\boldsymbol{\varepsilon}_q$ are activated in the image-space region and the Cartesian-space region respectively. Since both $\Delta\boldsymbol{\varepsilon}_x$ and $\Delta\boldsymbol{\varepsilon}_q$ are continuous, the control input of the manipulator $\boldsymbol{u}$ is also continuous without hard switching which is not desirable for cell manipulation.

The closed-loop equation is obtained by substituting the proposed controller in equation (22) into the dynamic model in equation (21) as:

$$\begin{aligned}&\boldsymbol{M}_q\dot{\boldsymbol{s}}_q+(\boldsymbol{B}_q+\boldsymbol{K}_s)\boldsymbol{s}_q+\boldsymbol{Y}_q(\dot{\boldsymbol{q}}_r, \ddot{\boldsymbol{q}}_r)\Delta\boldsymbol{\theta}_q \\ &+k_p(\beta_x\boldsymbol{J}^T(\boldsymbol{q})\Delta\boldsymbol{\varepsilon}_x+\beta_q\Delta\boldsymbol{\varepsilon}_q)=\mathbf{0}. \end{aligned} \quad (24)$$

A Lyapunov-like candidate is proposed as:

$$V=V_x+\tfrac{1}{2}\boldsymbol{s}_q^T\boldsymbol{M}(\boldsymbol{q})\boldsymbol{s}_q+P_I(\boldsymbol{p})+P_C(\boldsymbol{q})+\tfrac{1}{2}\Delta\boldsymbol{\theta}_q^T\boldsymbol{L}_q^{-1}\Delta\boldsymbol{\theta}_q. \quad (25)$$

Differentiating equation (25) with respect to time and substituting equations (7), (23) and (24) into it, we have:

$$\begin{aligned}\dot{V} &= -\dot{\boldsymbol{x}}^T(\boldsymbol{B}+\boldsymbol{K}_d)\dot{\boldsymbol{x}}+k\dot{\boldsymbol{x}}^T\Delta\boldsymbol{p} \\ &-\boldsymbol{s}_q^T(\boldsymbol{B}_q+\boldsymbol{K}_s)\boldsymbol{s}_q+k_p\beta_q\dot{\boldsymbol{p}}_a^T\boldsymbol{J}_I^{+T}(\boldsymbol{q})\Delta\boldsymbol{\varepsilon}_q - \\ &k_p(\beta_x\boldsymbol{J}_I^T(\boldsymbol{q})\Delta\boldsymbol{\varepsilon}_x+\beta_q\Delta\boldsymbol{\varepsilon}_q)^T(\beta_x\boldsymbol{J}_I^T(\boldsymbol{q})\Delta\boldsymbol{\varepsilon}_x+\beta_q\Delta\boldsymbol{\varepsilon}_q). \end{aligned} \quad (26)$$

The Cartesian-space region error $\Delta\boldsymbol{\varepsilon}_q$ is nonzero where $\boldsymbol{f}_c(\boldsymbol{q})>\mathbf{0}$, while the time derivative of the desired position input $\dot{\boldsymbol{p}}_d$ is nonzero where $\boldsymbol{f}_c(\boldsymbol{q})\leq\mathbf{0}$, as seen from equation (8). That is, $\Delta\boldsymbol{\varepsilon}_q$ and $\dot{\boldsymbol{p}}_d$ cannot be nonzero at the same time. From the definition of $\dot{\boldsymbol{p}}_a$, $\Delta\boldsymbol{\varepsilon}_q$ and $\dot{\boldsymbol{p}}_a$ cannot be nonzero at the same time either. Therefore, $\dot{\boldsymbol{p}}_a^T\boldsymbol{J}_I^{+T}(\boldsymbol{q})\Delta\boldsymbol{\varepsilon}_q = 0$, and equation (26) becomes:

$$\begin{aligned}\dot{V} &= -\dot{\boldsymbol{x}}^T(\boldsymbol{B}+\boldsymbol{K}_d)\dot{\boldsymbol{x}}+k\dot{\boldsymbol{x}}^T\Delta\boldsymbol{p}-\boldsymbol{s}_q^T(\boldsymbol{B}_q+\boldsymbol{K}_s)\boldsymbol{s}_q \\ &-k_p(\beta_x\boldsymbol{J}_I^T(\boldsymbol{q})\Delta\boldsymbol{\varepsilon}_x+\beta_q\Delta\boldsymbol{\varepsilon}_q)^T(\beta_x\boldsymbol{J}_I^T(\boldsymbol{q})\Delta\boldsymbol{\varepsilon}_x+\beta_q\Delta\boldsymbol{\varepsilon}_q). \end{aligned} \quad (27)$$

Note that $k\dot{\boldsymbol{x}}^T\Delta\boldsymbol{p} \leq \frac{k}{2}(\dot{\boldsymbol{x}}^T\dot{\boldsymbol{x}}+\Delta\boldsymbol{p}^T\Delta\boldsymbol{p})$. If the control parameters are set such that:

$$\begin{aligned}&k_p(\beta_x\boldsymbol{J}_I^T(\boldsymbol{q})\Delta\boldsymbol{\varepsilon}_x+\beta_q\Delta\boldsymbol{\varepsilon}_q)^T(\beta_x\boldsymbol{J}_I^T(\boldsymbol{q})\Delta\boldsymbol{\varepsilon}_x+\beta_q\Delta\boldsymbol{\varepsilon}_q) \\ &\geq \tfrac{k}{2}\Delta\boldsymbol{p}^T\Delta\boldsymbol{p}, \end{aligned} \quad (28)$$

$$\lambda_{min}[\boldsymbol{B}+\boldsymbol{K}_d] \geq \tfrac{k}{2}, \quad (29)$$

where $\lambda_{min}[\bullet]$ is the minimum eigenvalue, then $\dot{V} \leq 0$. We can now state the following theorem:

Theorem: *The robotic control law (22) and the update law (23) for the optical tweezers system guarantee the convergence of manipulation task, that is, $\boldsymbol{x} \rightarrow \boldsymbol{x}_d$, and $\boldsymbol{p} \rightarrow \boldsymbol{p}_d$ as $t \rightarrow \infty$, if the control parameters are chosen such that the conditions (28) and (29) are satisfied.*

Proof: If the conditions (28) and (29) are satisfied, we have $V>0$ and $\dot{V}\leq 0$, and hence V is bounded. Therefore, $\dot{\boldsymbol{x}}$, $\boldsymbol{s}_q$, $\Delta\boldsymbol{\theta}_q$, $\Delta\boldsymbol{x}$, $P_I(\boldsymbol{p})$, and $P_C(\boldsymbol{q})$ are bounded. The boundedness of $\Delta\boldsymbol{x}$ ensures the boundedness of $\boldsymbol{x}$ since $\Delta\boldsymbol{x}=\boldsymbol{x}-\boldsymbol{x}_d$. The boundedness of $P_I(\boldsymbol{p})$ and $P_C(\boldsymbol{q})$ ensures the boundedness of $f_t(\boldsymbol{p})$, $f_h(\boldsymbol{p})$ and $\boldsymbol{f}_c(\boldsymbol{q})$. Since the region functions are

bounded, the variables $\boldsymbol{p}$ and $\boldsymbol{q}$ are bounded. Therefore, the region errors $\Delta\boldsymbol{\varepsilon}_q$ and $\Delta\boldsymbol{\varepsilon}_x$ are bounded. In addition, the boundedness of $\dot{\boldsymbol{x}}$, $\boldsymbol{x}$, and $\boldsymbol{p}$ ensures the boundedness of $\ddot{\boldsymbol{x}}$ from equation (1). Differentiating equation (4) with respect to time, it is obtained that $\dot{\boldsymbol{p}}_d$ is bounded. Therefore, $\dot{\boldsymbol{q}}_r$ is also bounded since $\Delta\boldsymbol{\varepsilon}_q$, $\Delta\boldsymbol{\varepsilon}_x$, $\dot{\boldsymbol{p}}_d$ and $\boldsymbol{p}$ are bounded. From equation (20), $\dot{\boldsymbol{q}}$ is bounded because $\boldsymbol{s}_q$ and $\dot{\boldsymbol{q}}_r$ are bounded. The boundedness of $\dot{\boldsymbol{q}}$ guarantees the boundedness of $\dot{\boldsymbol{p}}$ since $\boldsymbol{J}_I(\boldsymbol{q})$ is a trigonometric function of $\boldsymbol{q}$ or constant. Therefore, the term $\beta_x\boldsymbol{J}_I^T(\boldsymbol{q})\Delta\boldsymbol{\varepsilon}_x+\beta_q\Delta\boldsymbol{\varepsilon}_q$ is uniformly continuous. From equation (27), it is easy to verify that $\beta_x\boldsymbol{J}_I^T(\boldsymbol{q})\Delta\boldsymbol{\varepsilon}_x+\beta_q\Delta\boldsymbol{\varepsilon}_q \in L_2(0,+\infty)$. Then it follows [25]–[27] that:

$$\beta_x\boldsymbol{J}_I^T(\boldsymbol{q})\Delta\boldsymbol{\varepsilon}_x+\beta_q\Delta\boldsymbol{\varepsilon}_q \rightarrow \boldsymbol{0}. \tag{30}$$

If the laser beam is located outside the image-space region where $f_h(\boldsymbol{p})>0$, we have $\Delta\boldsymbol{\varepsilon}_q \neq \boldsymbol{0}$ and $\Delta\boldsymbol{\varepsilon}_x = \boldsymbol{0}$, which contracts with equation (30) since $\boldsymbol{J}_I(\boldsymbol{q})$ is non-singular. If the laser beam is located in the overlapping area where $\boldsymbol{f}_c(\boldsymbol{q})>\boldsymbol{0}$ and $f_h(\boldsymbol{p})\leq 0$, we have $\Delta\boldsymbol{\varepsilon}_x \neq \boldsymbol{0}$ and $\Delta\boldsymbol{\varepsilon}_q \neq \boldsymbol{0}$. Since the gradient of potential energy is not zero, the laser beam cannot stay in the overlapping area.

Therefore, the laser beam can only settle down where $\boldsymbol{f}_c(\boldsymbol{q})\leq 0$ and thus $f_t(\boldsymbol{p})\leq 0$. That is, $\Delta\boldsymbol{\varepsilon}_q=\boldsymbol{0}$. Since $\boldsymbol{J}_I(\boldsymbol{q})$ is non-singular, $\Delta\boldsymbol{\varepsilon}_x=\boldsymbol{0}$ from equation (30). From equation (14), $\Delta\boldsymbol{\varepsilon}_x=\boldsymbol{0}$ can only be satisfied where $f_t(\boldsymbol{p}) \leq 0$, and hence $\Delta\boldsymbol{\varepsilon}_x=\boldsymbol{0}$ means that $\frac{\partial f_t(\boldsymbol{p})}{\partial \Delta \boldsymbol{p}} = \boldsymbol{0}$. That is, $\boldsymbol{p} \rightarrow \boldsymbol{p}_d$ as $t \rightarrow \infty$. The convergence of $\boldsymbol{p} \rightarrow \boldsymbol{p}_d$ then guarantees that $\boldsymbol{x} \rightarrow \boldsymbol{x}_d$ and $\dot{\boldsymbol{x}} \rightarrow \boldsymbol{0}$ as $t \rightarrow \infty$. △△△

Remark 2: Since the trapping stiffness k is very small and the gradient of the potential energy $\beta_x\boldsymbol{J}_I^T(\boldsymbol{q})\Delta\boldsymbol{\varepsilon}_x+\beta_q\Delta\boldsymbol{\varepsilon}_q$ is nonzero until the the actual position $\boldsymbol{p}$ reaches the desired position $\boldsymbol{p}_d$, the control parameters k_p, β_x, and β_q can be chosen sufficiently large such that condition (28) is satisfied. △△△

V. Experiment

The proposed control method was implemented in a robot-tweezer manipulation system in the City University of Hong Kong, as shown in Fig. 2. The system is constituted of three modules for sensing, control and execution [11]. The sensing module consists of a microscope and a CCD camera, and the position of the cell can be obtained through image processing. The control module consists of a phase modulator and a stepping motor controller. The execution module consists of the holographic optical trapping and the motorized stage. The mechanical components are supported by an anti-vibration table in a clean room. The optical tweezers were controlled to manipulate the yeast cell, and the relationship between the Cartesian space and the image space is known as 0.11 μm/pixel.

To illustrate the performance of the proposed control method, the positions of the laser beam and the trapped cell were intentionally moved outside the FOV as shown in Fig. 3. A yeast cell was manipulated by the laser from the position $(13.3, 37.0)$ μm inside the Cartesian-space region (outside FOV) to a desired position at $(400, 300)$ pixel within the image-space region (inside FOV) as shown in Fig. 3.

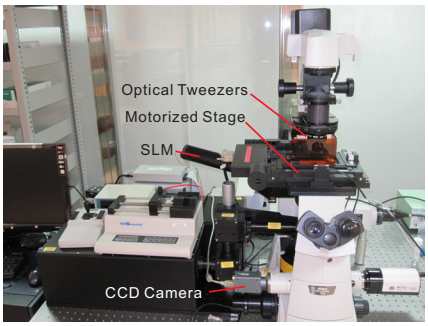

Fig. 2. A robot-tweezer manipulation system.

The task-oriented image-space region $f_t(\boldsymbol{p})$ was formulated to enclose the desired position $\boldsymbol{p}_d$, and the parameters of the region in equation (9) were set as: $p_{b1}=300$ pixel if $p_1 \leq p_{d1}$ else $p_{b1} = 500$ pixel; $p_{b2} = 200$ pixel if $p_2 \leq p_{d2}$ else $p_{b2} = 400$ pixel. Next, the high-order image-space region $f_h(\boldsymbol{p})$ was formulated to match the FOV, and the parameters of the region in equation (11) were set as: $n_h=20$, and $\kappa=0.7$. To drive the laser back to the FOV, the Cartesian-space region $\boldsymbol{f}_c(\boldsymbol{q})$ in equation (17) was specified as: $[q_{f1}, q_{f2}]^T=[60, 33]^T$ μm, $q_{b1}=36.3$ μm if $q_1 \leq q_{f1}$ else $q_{b1}=51.7$ μm; $q_{b2}=25.3$ μm if $q_2 \leq q_{f2}$ else $q_{b2} = 40.7$ μm. Note that the Cartesian-space region is specified in 2-D space, since the laser beam evolves in the 2-D plane of the stage while the camera is perpendicular to the evolving plane of the laser beam. The visual feedback is employed where $f_t(\boldsymbol{p})\leq 0$ and $f_h(\boldsymbol{p})\leq 0$, and the Cartesian-space feedback is employed where $\boldsymbol{f}_c(\boldsymbol{q})>0$.

The control parameters in equation (22) were set as: $\boldsymbol{K}_s=diag\{0.2,0.2\}$, $\beta_x=5$, $\beta_q=10$, $k_p=1$, $k_h=2$, $k_t=1$, $k_{r1}=k_{r2}=1$, and $\boldsymbol{L}_q=diag\{0.0001,0.0001\}$. The path of the laser and the cell in Cartesian space was shown in Fig. 4(a), and the path in image space was shown in Fig. 4(b). It is seen that the laser beam moves from the Cartesian-space region back to the image-space region and converges to the desired position within the image-space region. The position error is shown in Fig. 4(c), which converges to zero in about 3 s.

VI. Conclusions

In this paper, a new robotic manipulation technique has been developed for optical manipulation with the limited FOV. The proposed control strategy consists of a visual feedback control that ensures the convergence of position error inside the FOV and a Cartesian-space feedback control that drives the laser beam back to the FOV. The smooth combination of the Cartesian-space feedback and the visual feedback allows the laser beam to leave the FOV during the course of manipulation, such that the problem of the limited FOV is resolved. Experimental results have been presented to illustrate the performance of the proposed control method.

References

[1] M. Rakotondrabe, and I. A. Ivan, "Development and force/position control of a new hybrid thermo-piezoelectric microgripper dedicated

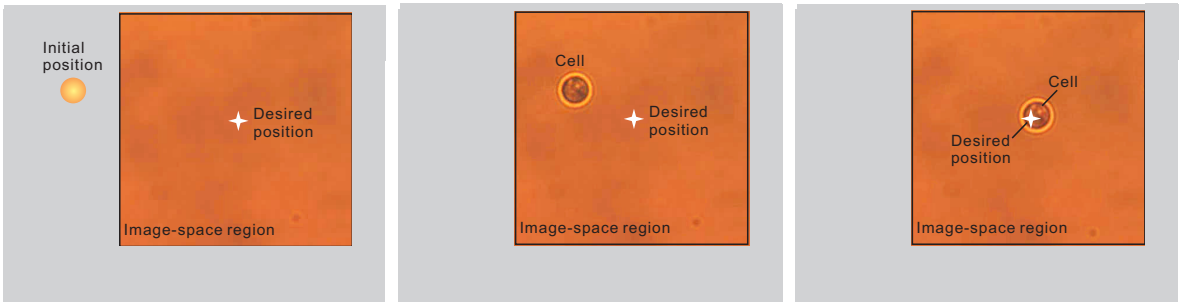

(a) t=0 s (b) t=1 s (c) t=4 s

Fig. 3. Experiment 1: Both the laser and the cell move from outside to inside the FOV.

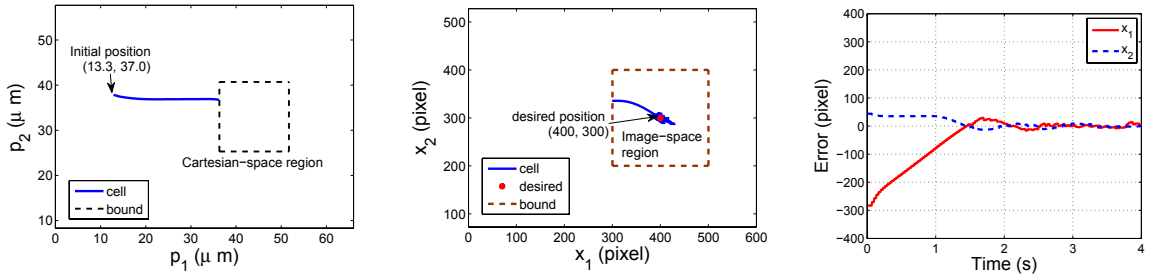

(a) path in Cartesian space (b) path in image space (c) position error

Fig. 4. Experiment 1: Both the laser and the cell move from $(13.3, 37.0)$ μm in Cartesian space (outside FOV) to the desired position at $[p_{d1}, p_{d2}]^T = [400, 300]^T$ pixel in image space (inside FOV).

to micromanipulation tasks," *IEEE Trans. Autom. Sci. Eng.*, Vol. 8, No. 4, pp. 824-834, 2011.

[2] Y. Sun, and B. J. Nelson, "Biological cell injection using an autonomous microrobotic system," *Int. J. Robotics Res.*, 21(10-11), 861-868, 2002.

[3] H. Huang, D. Sun, J. K. Mills, and S. H. Cheng, "Robotic cell injection system with position and force control: toward automatic batch biomanipulation," *IEEE Trans. Robotics*, 25(3), 727-737, 2009.

[4] X. Zhang, C, Leung, Z. Lu, N. Esfandiari, R. F. Casper, and Y. Sun, "Controlled aspiration and positioning of biological cells in a micropipette," *IEEE Trans. Biomed. Eng.*, 59(4), 1032-1040, 2012.

[5] A. Ashkin, J. M. Dziedzic, J. E. Bjorkholm, and S. Chu, "Observation of a single beam gradient force optical trap for dielectric particles," *Opt. Letters*, Vol. 11, pp. 288-290, 1986.

[6] A. Ranaweera, and B. Bamieh, "Modeling, identification and control of a spherical particle trapped in an optical tweezer," *Int. J. Robust Nonlin.*, Vol. 15, No. 16, pp. 747-768, 2005.

[7] A. E. Wallin, H. Ojala, E. Haggstrom, and R. Tuma, "Stiffer optical tweezers through real-time feedback control," *Applied Physics Letters*, Vol. 92, 2008.

[8] J. Wan, Y. Huang, S. Jhiang, and C. H. Menq, "Real-time *in situ* calibration of an optically trapped probing system," *Appl. Opt.*, Vol. 48, No. 25, pp. 4832-4841, 2009.

[9] Y. Huang, Z. Zhang, and C. H. Menq, "Minimum-variance brownian motion control of an optically trapped probe," *Appl. Opt.*, Vol. 48, No. 3, pp. 5871-5880, 2009.

[10] C. Aguilar-Ibanez, M. S. Suarez-Castanon, and L. I. Rosas-Soriano, "A simple control scheme for the manipulation of a particle by means of optical tweezers," *Int. J. Robust Nonlin.*, 21(3), 328-337, 2010.

[11] S. Hu, and D. Sun, "Automatic transportation of biological cells with a robot-tweezer manipulation system," *Int. J. Robotics Res.*, Vol. 30, No. 14, pp. 1681-1694, 2011.

[12] Y. Huang, P. Cheng, and C. H. Menq, "Dynamic force sensing using an optically trapped probing system," *IEEE/ASME Trans. Mech.*, Vol. 16, No. 6, pp. 1145-1154, 2011.

[13] H. Chen, and D. Sun, "Moving groups of microparticles into array with a robot-tweezers manipulation system," *IEEE Trans. Robotics*, Vol. 28, No. 5, pp. 1069-1080, 2012.

[14] Y. Wu, D. Sun, W. Huang, and N. Xi, "Dynamics analysis and motion planning for automated cell transportation with optical tweezers," *IEEE/ASME Trans. Mech.*, Vol. 18, No. 2, pp. 706-713, 2013.

[15] X. Li, C. C. Cheah, S. Hu, and D. Sun, "Dynamic trapping and manipulation of biological cells with optical tweezers," *Automatica*, Vol. 49, No. 6, 1614-1625, 2013.

[16] N. Garcia-Aracil, E. Malis, R. Aracil-Santonja, and C. Perez-Vidal, "Continuous visual servoing despite the changes of visibility in image features," *IEEE Trans. Robotics*, Vol. 21, No. 6, pp. 1214-1220, 2005.

[17] N. R. Gans, G. Hu, K. Nagarajan, and W. E. Dixon, "Keeping multiple moving targets in the field of view of a mobile camera," *IEEE Trans. Robotics*, Vol. 27, No. 4, pp. 822-828, 2011.

[18] X. Li, and C. C. Cheah, "Global task-space adaptive control of robot," *Automatica*, Vol. 49, No. 1, pp. 58-69, 2013.

[19] X. Li, and C. C. Cheah, "Dynamic region control for robot-assisted cell manipulation using optical tweezers," *IEEE Int. Conf. Robotics Automat.*, pp. 1057-1062, 2012.

[20] S. Hutchinson, G. Hager, and P. Corke, "A tutorial on visual servo control," *IEEE Trans. Robotics Automat.*, 12(5), 651-670, 1996.

[21] Y. H. Liu, H. Wang, C. Wang, and K. K. Lam, "Uncalibrated visual servoing of robots using a depth-independent interaction matrix," *IEEE Trans. Robotics*, Vol. 22, No. 4, pp. 804-817, 2006.

[22] B. Espiau, F. Chaumette, and P. Rives, "A new approach to visual servoing in robotics," *IEEE Trans. Robotics Automat.*, Vol. 8, No. 3, pp. 313-326, 1992.

[23] L. E. Weiss, A. C. Sanderson, and C. P. Neuman, "Dynamic sensor-based control of robots with visual feedback," *IEEE Trans. Robotics Automat.*, Vol. RA-3, No. 5, pp. 404-417, 1987.

[24] R. Steubling, S. Cheng, and M. W. Berns, "Laser-induced cell fusion in combination with optical tweezers: The laser-cell fusion trap," *Cytometry*, Vol. 12, No. 6, pp. 505-510, 1991.

[25] J. J. E. Slotine, and W. Li, *Applied Nonlinear Control*. Englewood Cliffs, New Jersy: Prentice Hall, 1991.

[26] S. Arimoto, *Control Theory of Nonlinear Mechanical Systems - A Passivity-Based and Circuit-Theoretic Approach*, Oxford, 1996.

[27] M. W. Spong, and M. Vidyasagar, *Robot Dynamics and Control*. New York: John Wiley & Sons, 1989.